Bull. Mater. Sci., Vol. 38, No. 5, September 2015, pp. 1291–1299. © Indian Academy of Sciences.

Growth and characterization of nonlinear optical single crystals: bis(cyclohexylammonium) terephthalate and cyclohexylammonium para-methoxy benzoate

P SATHYA, M ANANTHARAJA, N ELAVARASU and R GOPALAKRISHNAN*

Crystal Research Lab, Department of Physics, Anna University, Chennai 600 025, India

MS received 12 November 2014; accepted 30 April 2015

Abstract. Bis(cyclohexylammonium) terephthalate (BCT) and cyclohexylammonium 4-methoxy benzoate (C4MB) single crystals were successfully grown by the slow evaporation solution growth technique. The harvested crystals were subjected to single-crystal X-ray diffraction, spectral, optical, thermal and mechanical studies in order to evaluate physiochemical properties. The Kurtz and Perry technique for second harmonic generation (SHG) study revealed that the powdered materials of BCT and C4MB exhibit SHG efficiency 0.2 times less and 1.3 times greater than that of standard reference material potassium dihydrogen phosphate. C4MB crystal exhibits high efficiency than BCT, because of methoxy group substituted in the para position of phenyl ring. With high SHG efficiency and thermal stability para substituted C4MB crystal will be a potential candidate for optical device fabrication.

Keywords. Organic compound; growth from solution; characterization; nonlinear optical materials.

1. Introduction

Organic nonlinear optical (NLO) materials have attracted much attention due to their potential applications in telecommunication, optical switching, optical frequency conversion, THz generation, electro-optical and integrated optics.[1,2] In recent times, polar aromatic organic molecules have received great attention for NLO applications. However, NLO properties of several inorganic crystals such as $LiNbO_3$, GaP have been widely investigated. The NLO property in organic molecules mainly associates with polar functional group and large molecular hyperpolarizability, which are facilitated to electron delocalization. In addition to that the molecules should form noncentrosymmetrical crystal structure that provides nonvanishing second-order nonlinear coefficients.[3–5] By this way, hydrogen bonding, steric substitution and chirality molecules have also been proposed to crystallize into a noncentrosymmetric structure.[6]

Donor/acceptor benzene derivatives are demonstrated to produce high molecular nonlinearity. Till date many organic donor–π–acceptor (D–π–A) type compounds have been studied theoretically and also experimentally. Cyclohexylammonium 4-methoxy benzoate (C4MB) crystal is D–π–A type in organic molecules and expected to be a promising candidate for second harmonic generation (SHG).[7,8] The cyclohexylamine is new to crystal growth researchers and an interesting base material for different organic systems. It is a strong base and can easily react with all acids to form salts. Consequently the nitrogen atom in cyclohexylamine is extremely reactive on the organic compounds containing acid anhydrides. Hence, cyclohexylamine is selected to react with two different acids, i.e., terephthalic acid and para-methoxy benzoic acid. Both acids are having aromatic molecules and directional hydrogen bonds. Further, the numbers of carboxylic groups are placed at different positions of aromatic ring.[9] Here, methoxy (–OMe) group is substituted in a para position of phenyl ring which predicts an electron donating system and plays an important role in the crystal structure and SHG activity of the title compound.[10–12]

The present investigation gives the detailed results of growth, structural, optical, mechanical, thermal and NLO behaviour of the title compounds. It is interesting to study the new base–acid complex, bis(cyclohexylammonium) terephthalate (BCT) and cyclohexylammonium para-methoxy benzoate, which have been grown by the slow evaporation solution technique.

2. Experimental

2.1 *Synthesis and crystal growth of BCT and C4MB*

Cyclohexylamine, terephthalic acid and para-methoxy benzoic acid reagents were the starting materials used to synthesise the title compounds. BCT crystal was grown by

*Author for correspondence (krgkrishnan@yahoo.com, krgkrishnan@annauniv.edu)

reacting terephthalic acid and cyclohexylamine in the ratio of 1 : 2 in water solvent. Two protons are transferred from terephthalic acid to cyclohexylamine resulting in the formation of ions as depicted in figure 1. Similarly, C4MB was grown by mixing the cyclohexylamine and para-methoxy benzoic acid in equimolar ratio. Here a mixed solvent of water and ethanol were used to grow good quality crystals. The possible growth mechanism of C4MB is depicted in figure 2. The filtered solution was kept at 32°C and allowed for slow evaporation of solvents. Good quality transparent single crystals were harvested after a period of 4 weeks followed by recrystallization process. The grown crystals are shown in figure 3.

2.2 *Characterization techniques*

Crystal structure was confirmed by single-crystal X-ray diffraction (XRD) using ENRAF(BRUKER) NONIUS CAD 4 Kappa APEX II X-ray diffractometer equipped with MoKα radiation ($\lambda = 0.71073$ Å). The Fourier transform infrared (FT-IR) spectrum was recorded in the range 400–4000 cm^{-1} using KBr pellet on Bruker Alpha spectrometer. The number of protons and carbons present in

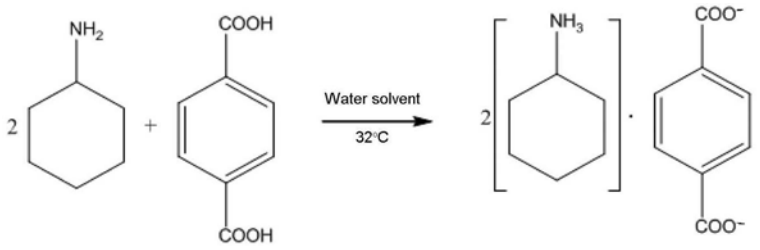

Figure 1. Reaction scheme of BCT.

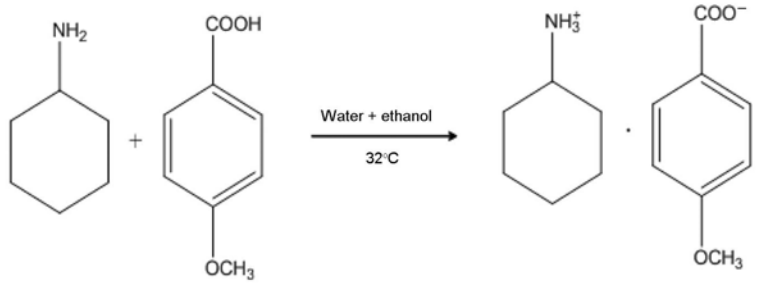

Figure 2. Reaction scheme of C4MB.

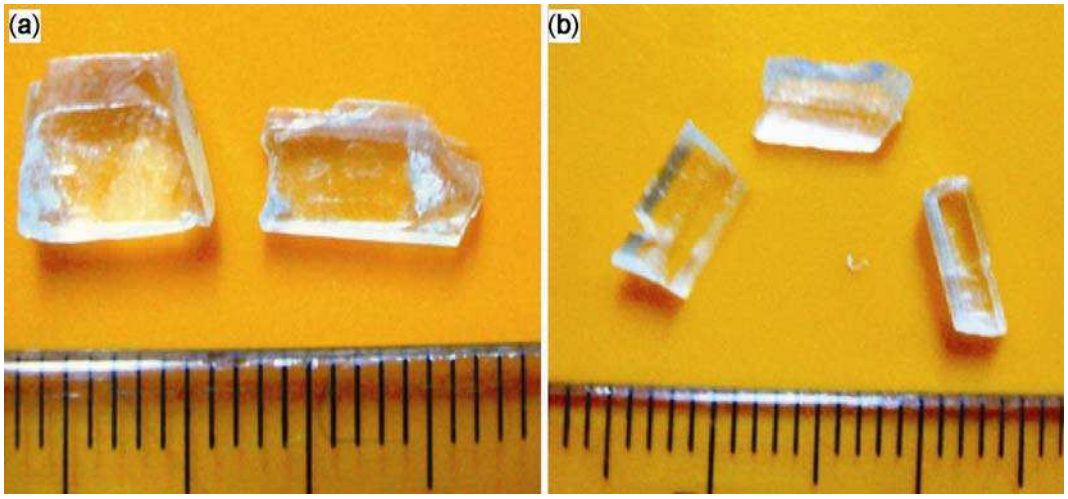

Figure 3. Single crystals of bis(cyclohexylammonium) terephthalate (crystal a) and cyclohexylammonium para-methoxy benzoate (crystal b).

the compounds were confirmed by FT-NMR 500 mHz analysis. Optical absorption spectral analysis was carried out using CARY 5E UV–vis spectrophotometer in the range of 200–800 nm. The fluorescence property of crystal was obtained using Fluorescence Spectrometer Perkin Elmer LS 45. The microhardness was tested by MATSUZAWA microhardness tester fitted with Vickers diamond pyramidal indenter attached to an incident light microscope. The thermogravimetric (TG) and differential thermal analyses (DTA) were made by NETZSCH STA 409°C analyser in the temperature range between 25 and 1000°C under nitrogen atmosphere with a heating rate of 10 K min^{-1}. The Kurtz and Perry powder technique was performed in order to obtain the SHG efficiency.

3. Results and discussion

3.1 *Single-crystal XRD analysis*

From single-crystal XRD data, it can be observed that BCT and C4MB crystals belong to monoclinic system with noncentrosymmetric space group (table 1). In the title compounds, cations and anions are linked by N–H…O hydrogen bonds between the H atoms of the ammonium group and the O atoms of the carboxylate group, which also make a great contribution to the stability of the crystal structure.[13,14] Both space groups of the title crystals reveal no inversion symmetry (noncentrosymmetry), hence they may exhibit SHG.

3.2 *FT-IR analysis*

FT-IR is a non-destructive microanalytical spectroscopy technique that involves understanding of molecular vibration and chemical bonding of the title compound. The beam of infrared radiation is passed through compounds. Molecular bonds and group of bonds vibrate by absorbing infrared energy at particular wavelengths.[15] BCT and C4MB are subjected to FT-IR studies. The resulting FT-IR spectrum is shown in figure 4. The results of BCT and C4MB are interpreted and presented in table 2. Para-methoxy group has been clearly observed at 847 cm^{-1} in the FT-IR spectrum of C4MB. In the C4MB crystal, the C=O stretching vibration occurs at 1741 cm^{-1} owing to the intramolecular hydrogen bonding and the presence of strong electronegative atom causing large degree of molecular, π-electron delocalization and redistribution of electrons, which weakens C=O bond.[16] Observed FT-IR spectra strongly confirm BCT and para-substituted C4MB crystals.

3.3 *Nuclear magnetic resonance (NMR) studies*

To confirm the molecular structure of BCT and C4MB crystal, the ^{1}H and ^{13}C NMR spectra were recorded using deuterated methanol as a solvent. BCT and C4MB crystals were crushed and dissolved in CD_3OD. Figure 5a and b, respectively, shows the ^{1}H NMR spectrum of BCT and C4MB. The multiplet peaks at 1.8, 1.4 ppm for BCT and 1.7, 1.4 ppm for C4MB are due to cyclic aliphatic proton in the cyclohexylamine. The sharp intense peak at 3.8 ppm is due to the protons in the methyl substituted benzoate. A sharp singlet peak at 5.1 ppm in both compounds is assigned for amine group (NH_3). Both the materials show the aromatic proton peak at 7.9 ppm (BCT) and 8.1, 7.1 ppm (C4MB). The strong intense peak at 3.8 ppm corresponds to the methoxy (–OMe) proton that either has relatively low electron density around it (electron donor groups) or that is attached to a carbon atom taking part in a π-bond.

The ^{13}C NMR spectra of BCT and C4MB are shown in figure 5c and d, respectively. The peaks at 24.52 and 30.65 ppm for both BCT and C4MB are due to aliphatic carbon. The resonance peak at 50.06 ppm in both the crystals is attributed to C atom in cyclohexane. The peak at $\delta = 54.37$ ppm for C4MB is mainly due to the methyl group. The NMR signals at 128.26 ppm (BCT) and 130.71, 112.53 ppm (C4MB) correspond to benzene ring carbon atoms. The resonance at 173.6 ppm in both compounds is due to carbonyl atom in acid functional group. Table 3 shows the ^{1}H and ^{13}C NMR spectra result of BCT and C4MB.

Table 1. Cell parameter values of BCT and C4MB.

	BCT		C4MB	
Crystal data	Obtained values	Reported values	Obtained values	Reported values
System	Monoclinic	Monoclinic	Monoclinic	Monoclinic
Space group	Cc	Cc	$P2_1$	$P2_1$
a (Å)	11.5839(3)	11.572(2)	8.91(18) Å	8.9076(18)
b (Å)	22.8008(5)	22.820(5)	6.62(12) Å	6.6025(13)
c (Å)	8.5272(16)	8.5426(17)	11.78(2) Å	11.778(2)
α, β, γ	$\alpha, \gamma = 90°, \beta = 117.0881°(3)$	$\beta = 117.03°(3)$	$\alpha, \gamma = 90°, \beta = 102.70(4)°$	$\beta = 102.85(3)°$
V	2005.1587 $Å^3$	2009.5(7) $Å^3$	678 $Å^3$	$V = 675.3(2)$ $Å^3$

Table 2. Assignment of vibrational frequencies of BCT and C4MB.

BCT wavenumber (cm^{-1})	C4MB wavenumber (cm^{-1})	Assignment
3445	3900, 3851, 3741	NH_3 asymmetrical stretching
2938, 2854	2937, 2853	C–H stretching
2191	2219	C≡N stretching
–	1741	C=O stretching
1634	1639	C=C stretching
1578	1521, 1587	Asymmetry COO^- stretching
1443	1449	C–C stretching in aromatic ring
1367, 1080	1372, 1098	C–N stretching in aromatic ring
–	1310	C–OCH_3 stretching
1135	1161	C–C–O stretching
1024	1028	C–H in plan bending
	847	C–H out of plan bending, para substituted
746	781	NH_3^+ rocking
–	611	C–C–O rocking
–	533	C–OCH_3 out of plan bending

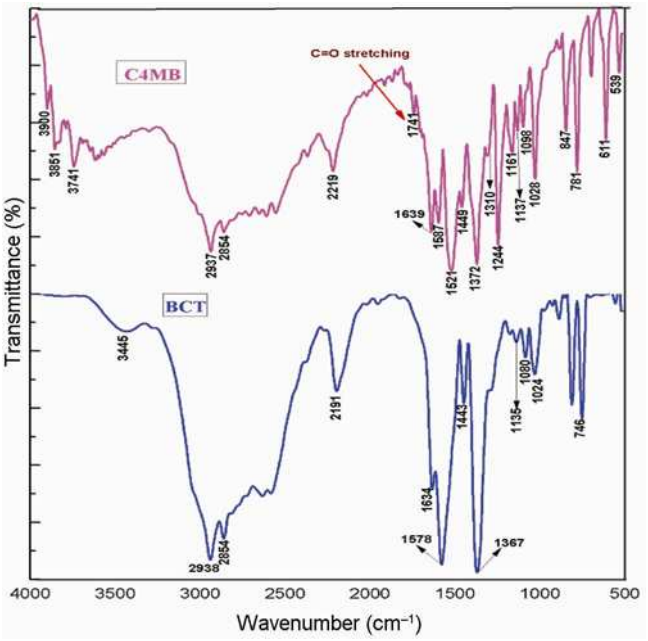

Figure 4. FT-IR spectrum of BCT and C4MB.

3.4 *UV–visible absorption spectrum*

In general UV–visible absorption in organic materials involves promotion of electrons between σ and π orbital from ground state to higher energy states.[17] Optical window width is an important property for NLO materials. Hence UV–visible absorption range of the title compound is necessary for optical applications. The BCT and C4MB crystals were well polished and subjected to UV–visible spectral analysis in the wavelength range 200–800 nm. Figure 6a and c shows the absorption spectrum of BCT and C4MB crystals. The cutoff wavelength was found to be 295 nm for BCT and 325 nm for C4MB owing to strong $\pi \rightarrow \pi^*$ electronic transition.[18] This band may be occurring in the aromatic ring C=O group.[19] The absence of energy absorption in the UV–visible absorption spectrum in entire visible region indicates the title crystals are desirable for NLO applications.

The optical absorption coefficient (α) of a crystal with different thicknesses can be calculated using the relation

$$\alpha = \frac{1}{d_2 - d_1} \times \ln\left(\frac{T_1}{T_2}\right),$$

where d_1 and d_2 are the two different thicknesses of the crystals and T_1 and T_2 are the transmittance of the crystal thickness d_1 and d_2, respectively.

The transmittance spectra of BCT crystals of thickness 3 and 2 mm were recorded, whereas for C4MB crystal, 3 and 1 mm thicknesses were used.

The optical bandgap energy is calculated from absorption spectra using the relation

$$\alpha h\nu = A(h\nu - E_g)^n,$$

where exponent $n = 1/2$ for direct allowed transition, $n = 3/2$ for direct forbidden transition, $n = 2$ for indirect allowed transition and for indirect forbidden transition $n = 3$; A is a constant, E_g is the optical bandgap, $h\nu$ the photon energy ($\nu = c/\lambda$). The optical bandgaps of the BCT and C4MB crystals were estimated by plotting $(\alpha h\nu)^{1/2}$ with $h\nu$ as shown in figure 6b and d. The indirect optical bandgap of grown BCT and C4MB crystals are found to be 3.8 and 3.7 eV, respectively. The values are obtained by extrapolating linear part of the absorption edge to the energy axis.

3.5 *Fluorescence studies*

Fluorescence property is used to determine the crystalline quality as well as its exciton fine structure. The

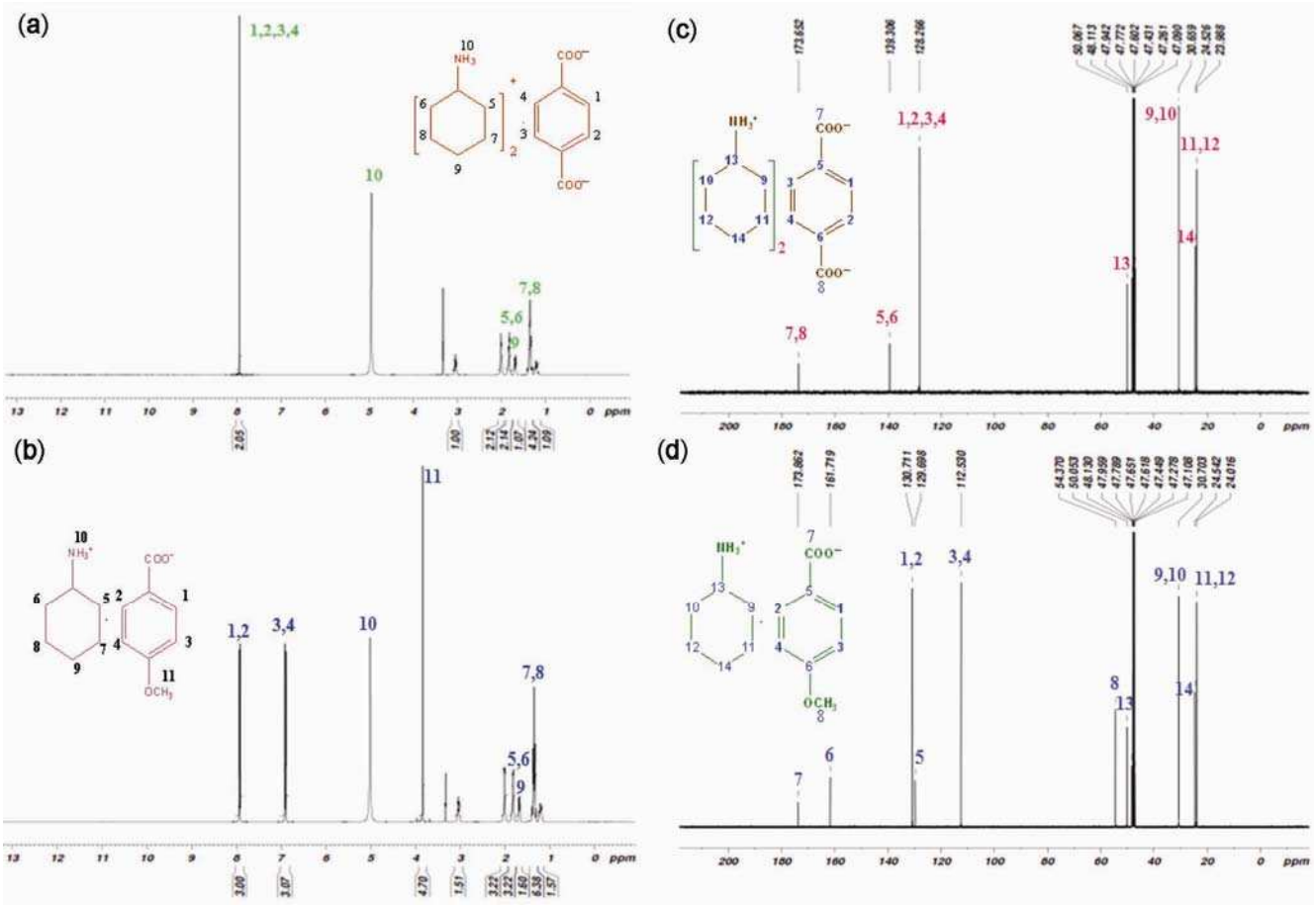

Figure 5. ^{1}H NMR spectrum of (**a**) BCT and (**b**) C4MB; and ^{13}C NMR spectrum of (**c**) BCT and (**d**) C4MB.

Table 3. ^{1}H and ^{13}C NMR spectra result of BCT and C4MB.

Spectrum	BCT Signal at δ ppm	C4MB Signal at δ ppm	Group identification
^{1}H	7.9	8.1, 7.1	Benzene ring (C–H, C–H, C–H, C–H) in acid (s)
	5.1	5.1	Amine (NH_3)
	3.2	3.3	Solvent
	2	2	Cyclohexane, aliphatic H atom 1 alpha N-form methane
	1.8, 1.4, 1.2	1.7, 1.4, 1.2	Aliphatic-H atom (multiplet)
		3.8	3 H atom on the methyl group of para-methoxy benzoic acid
^{13}C	173.6	173.8	Carbonyl, C atom in acid
	128.2	130.7, 112.5	C atom in the benzene ring
	50.0	50.3, 30	C atom in the cyclohexane
	139.3	129.6	Benzoate, C atom in the benzene ring
	23.9, 30.65	24.0, 30.7	Alpha, beta, gamma C from aliphatic, gamma N from aliphatic (C–C)
		54.37	Methyl group

fluorescence emission spectra for BCT and C4MB crystal samples were recorded in the range from 400 to 600 nm at excitation wavelength 400 and 520 nm, respectively. The fluorescence spectra of both crystals are given in figure 7. The emission was assigned to the electronic transition from π^* antibonding molecular orbital to π bonding molecular orbital of both crystals. The higher intensity ratio indicates purity and perfect crystallinity of the title compounds. Hence, both crystals are suitable for optoelectronic laser devices.

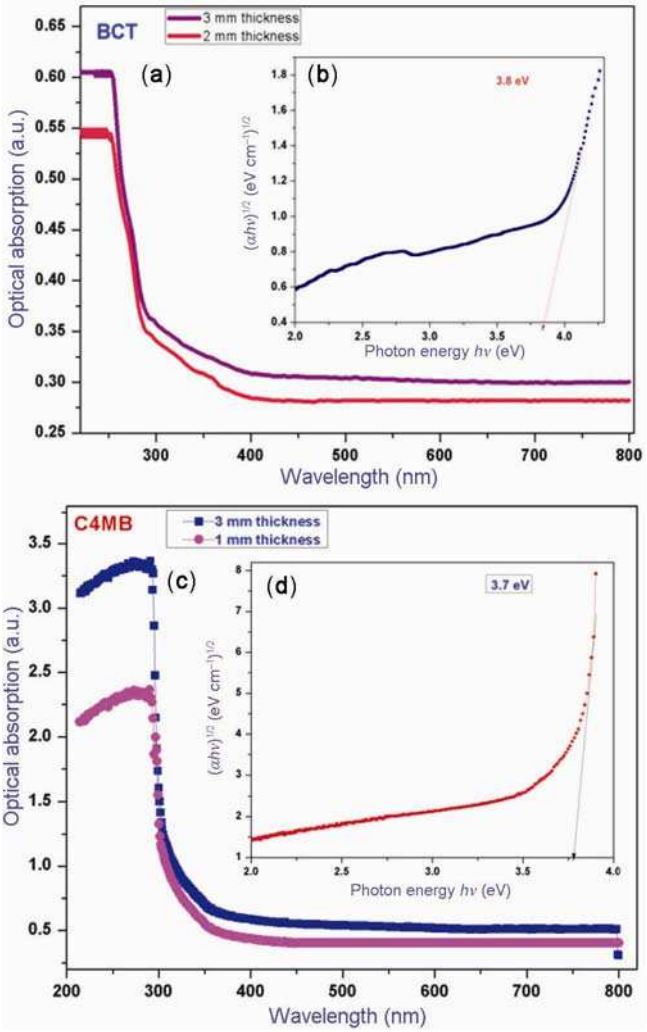

Figure 6. (**a**, **b**) Plot of UV–visible absorption spectrum and bandgap of BCT crystal and (**c**, **d**) C4MB crystal.

3.6 *Hardness test*

Mechanical stability of organic single crystal is very important for device fabrication. Vickers microhardness tests were performed on the grown crystals with flat and smooth faces for applied loads 5, 10, 25 and 50 g. The indentation time was kept constant as 5 s for each load. Vickers microhardness H_V was computed using the relation $H_V = 1.8544P/d^2$ kg mm^{-2}, where P is applied load in kg and d is indentation diagonal length in mm. A graph was plotted between hardness number (H_V) and applied load (P) as shown in figure 8a. The hardness of BCT and C4MB crystals increases with increasing load, which indicates the reverse indentation size effect (RISE). Above 50 g crakes were observed owing to release of internal stresses generated locally by indentation. The RISE occurs in crystals which undergo plastic deformation. The RISE can be caused in two ways (i) the relative predominance of nucleation and multiplication of dislocations

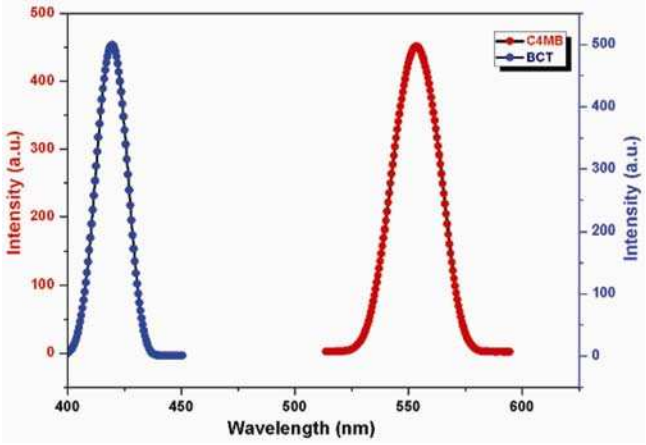

Figure 7. Fluorescence spectrum of BCT and C4MB.

and (ii) the relative predominance of activity either two sets of slip planes of a particular slip system or two slip systems below and above a particular load.[20]

Meyer's index number (n) can be calculated from the Meyer's law

$$P = kd^n,$$

$$\log P = \log k + n \log d.$$

From the careful observations, Onitsch[21] and Hanneman[22] pointed out that n lies between 1 and 1.6 for moderately hard materials and it is more than 1.6 for soft materials. The slope of the graph plotted between $\log P$ *vs.* $\log d$ (figure 8b) gives Meyer's index number (n). The value of n obtained for BCT is 2.6 and C4MB is 2.4. Hence both crystals belong to soft material category.

Elastic stiffness constant gives the idea of tightness of bonding between neighbouring atoms.[23] The stiffness constant (C_{11}) is calculated from Wooster's empirical relation[24] given by

$$C_{11} = H_V^{7/4}.$$

The variation of stiffness constant (C_{11}) with various loads is shown in figure 8c.

The yield strength (σ_y) was calculated from hardness values. The yield strength depends on Meyer's index number n. For $n > 2$, σ_y can be calculated using the relation

$$\sigma_y = \frac{3-n}{2.9}\left(\frac{[12.5(n-2)]}{3-n}\right)^{n-2} H_V.$$

For $n < 2$, the yield strength is calculated using the expression

$$\sigma_y = \frac{H_V}{3}.$$

From figure 8d, it is observed that yield strength increases with increasing load.

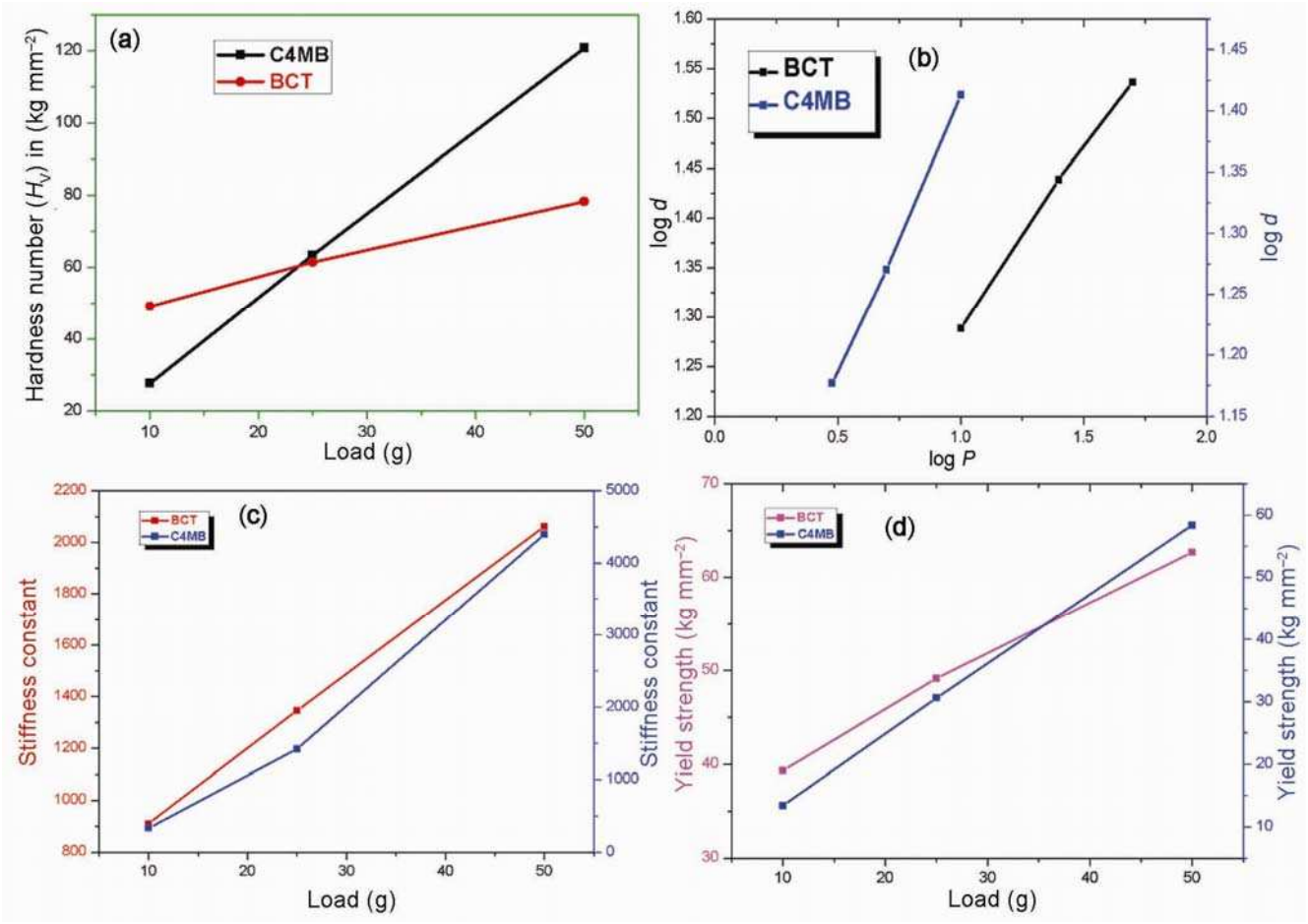

Figure 8. (**a**) Vickers microhardness test curve for BCT and C4MB. (**b**) plot of log *P vs.* log *d* for BCT and C4MB crystals. (**c**) Variation of stiffness constant with load of BCT and C4MB crystals and (**d**) Variation of yield strength with load of BCT and C4MB crystals.

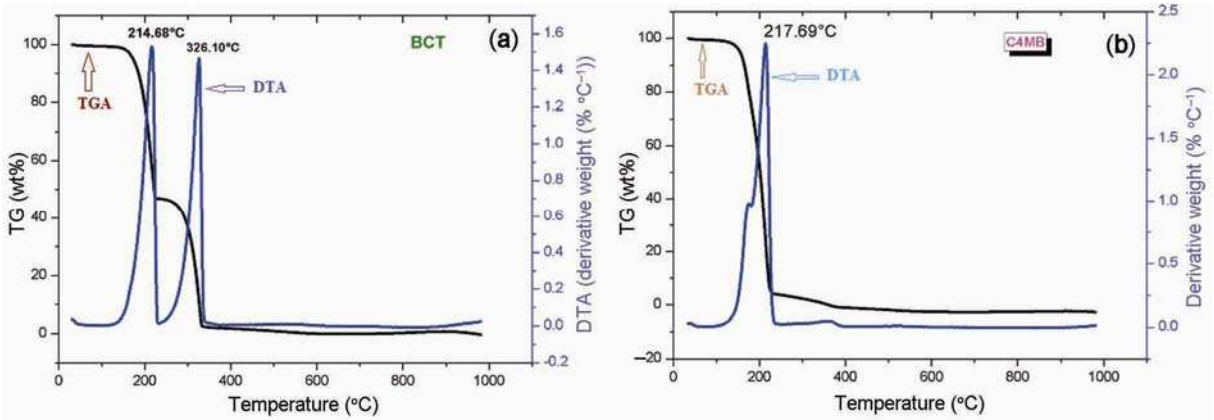

Figure 9. Thermal analysis curves of (**a**) BCT and (**b**) C4MB.

3.7 *Thermal analysis*

Thermograms provide information about decomposition patterns and weight loss of the materials. Differential thermal analysis (DTA) curve gives information regarding the phase transformations, water of crystallization and melting point of the compound.[25]

TG/DTA curves of BCT and C4MB are shown in figure 9. In DTA curve both the compounds exhibit sharp exothermic peak at 214.6 and 217.6°C which are attributed to meting point of the BCT and C4MB, respectively. The second exothermic peak in DTA curve at 326°C indicates that the material is fully decomposed. The sharpness of exothermic peaks infers the good degree of

Table 4. SHG output for BCT and C4MB.

Input energy	KDP	BCT	C4MB
680 mJ	2.5 mV	2.2 mV	3.8 mV

crystallinity of grown samples. The DTA curve of BCT crystal has two exothermic peaks, which are due to two carboxylate ester that decomposed at two different temperatures, whereas for C4MB crystal one carboxylate ester completely decomposed at 217°C. From TGA curves, it is observed that BCT is thermally stable up to 189.65°C and C4MB up to 154.26°C. There is no phase transition till the title materials decompose.

3.8 *NLO studies*

The SHG conversion efficiency of the compound was measured by the Kurtz and Perry[26] powder technique. The efficiency of the energy (frequency) conversion is confirmed by the emission of green light from the powder sample. Input power of laser is 680 mJ and pulse width of 8 ns and repetition rate of 10 Hz. The input laser beam was passed through an IR reflector to the sample. Photodiode and oscilloscope were assembled to detect the light emitted by samples. The output power is measured as 2.5 mV for potassium dihydrogen phosphate (KDP) crystal. For the same input, BCT and C4MB samples emitted the green light with the output power of 2.2 and 3.8 mV, respectively (table 4). It is inferred that the C4MB compound exhibits a reasonable SHG output, where methoxy (–OMe) group substitutes in the para position of phenyl ring, when compared to BCT crystal which exhibits less SHG efficiency.

4. Structural relationship

Crystal structure of the both materials suggests the intermolecular charge transfer from the carboxyl hydrogen to the nitrogen atom of the bases through hydrogen bond interactions. The hydrogen bond conjugated path can induce large molecular dipole moment and molecular polarizability of the title compounds, which yield NLO efficiency. In the C4MB crystal, very week intramolecular hydrogen bonds between C–H (methyl) groups as proton donors, and the N, O atoms and the π electrons of the aromatic ring as the proton acceptors promote the high SHG signal. And also, methyl groups substituted in para position of phenyl ring are non-planar, which predicts maximum conjugation of molecule with donor and acceptor groups. But in the case of BCT crystal, only the N–H…O intermolecular interaction takes place, which emphasize its lessor SHG efficiency than C4MB. The main reasons to get high SHG efficiency in C4MB crystal is both inter- and intramolecular hydrogen bonds in the molecules.[27] Hence C4MB crystalline powder exhibits high SHG efficiency compared to BCT compound.

5. Conclusion

BCT and C4MB crystals were grown by the slow evaporation solution technique for the present investigation. The unit cell parameters were confirmed by single-crystal XRD analysis. FT-IR spectrum clearly confirmed the presence of various functional groups present in both the crystals. NMR studies confirmed the placing of proton and carbon in the BCT and C4MB molecules. From UV–vis spectral analysis, it is observed that crystals have good transparency in the entire visible region. Fluorescence spectrum shows the broad emission peaks at 422 and 558 nm, respectively, for BCT and C4MB crystals. From the Vickers microhardness test, hardness number (H_V), yield strength (σ_y) and elastic stiffness constant (C_{11}) were calculated. The Vickers microhardness studies show the RISE and both crystals are categorized under soft materials. The crystals are thermally stable up to 190 and 154°C for BCT and C4MB, respectively. Cyclohexylammonium p-methoxy benzoate molecule has a methyl group as proton donor, and the N, O atoms and the π electrons of the aromatic ring as the proton acceptors to induce SHG character. The Kurtz and Perry powder technique reveals the C4MB crystalline powder exhibits high nonlinearity due to strong intermolecular hydrogen bond.

References

1. Nakanishi H, Matsuda H, Okada S and Kato M 1989 *Adv. Mater.* **1** 97
2. Matsukawa T, Yoshimura M, Takahashi Y, Takemoto Y, Takeya K, Kawayama I, Okada S, Tonouchi M, Kitaoka Y, Mori Y and Sasaki T 2010 *Jpn. J. Appl. Phys.* **49** 075502
3. Shivachev B L, Kossev K, Dimowa L T, Yankov G, Petrov T, Nikolova R P and Petrova N 2013 *J. Cryst. Growth* **376** 41
4. Thomas Joseph Prakash J and Gnanaraj M S 2015 *J. Spectrochem. Acta, Part A: Mol. Biomol. Spectrosc.* **135** 39
5. Jha P C, Anusooya Pati Y and Ramasesha S 2005 *Mol. Phys.* **103** 1859
6. Ukachi T, Shigemoto T, Komatsu H and Sugiyama T 1993 *J. Opt. Soc. Am. B* **10** 1372
7. Yang Z, Aravazhi S, Schneider A, Seiler P, Jazbinsek M and Gunter P 2005 *Adv. Funct. Mater.* **15** 1072
8. Ravindra H J, John Kiran A, Dharmaprakash S M, Satheesh Rai N, Chandrasekharan K, Kalluraya B and Rotermund F 2008 *J. Cryst. Growth* **310** 4169
9. Zhao P S, Wang X, Jian F F, Zhang J L and Xiao H L 2010 *J. Serb. Chem. Soc.* **75** 459
10. Suresh S 2013 *Br. J. Appl. Sci. Technol.* **3** 340
11. Patil P S, Bhumannavar V M, Bannur M S, Kulkarni H N and Bhagavannarayana G 2013 *J. Cryst. Process. Technol.* **3** 108
12. Tam W, Cheng L-T, Bierleinl J D, Cheng L K, Wang Y, Feiring A E, Meredith G R, Eaton D F, Calabrese J C and Rikken G L J A 1991 *ACS Symp. Series* **455** 158

13. Han M T 2012 *Acta Crystallogr*. **68** 1579
14. Wei B 2011 *Acta Crystallogr*. **67** 2185
15. Stuart B H 2005 *Infrared spectroscopy: fundamentals and applications, analytical technique in the science*, doi: 10.1002/0470011149
16. Sajan D, Hubert Joe I and Jayakumar V S 2006 *J. Phys.: Conf. Ser*. **28** 123
17. Sankar R, Raghavan C M, Balaji M, Kumar R M and Jayavel R 2007 *Cryst. Growth Des*. **7** 348
18. Josepha L, Sajana D, Shettigar V, Chaitanya K, Tom Sundius N M and Nemec I 2013 *Mater. Chem. Phys*. **141** 248
19. Waghmare V G, Kariya K P and Paliwal L J 2011 *Mater. Sci. Eng. B* **1** 485
20. Sangwal K 2000 *Mater. Chem. Phys*. **63** 145
21. Onitsch E M 1947 *Mikroskopie* **2** 131
22. Hanneman M 1941 *Metall. Manch* **23** 135
23. Khalil S M 2012 *AIP Adv*. **2** 042183
24. Wooster W A 1953 *Rep. Prog. Phys*. **16** 16
25. Meng F Q, Lu M K, Yang Z H and Zeng H 1998 *Mater. Lett*. **33** 265
26. Kurtz S K and Perry T T 1968 *J. Appl. Phys*. **39** 3798
27. Rappoport Z 2007 *The chemistry of aniline* (England: Wiley) p 1807